

# STAR Highlights

– 2024 RHIC/AGS annual users' meeting

Yicheng Feng  
(for the STAR Collaboration)

Purdue University

June 13, 2024



**PURDUE**  
UNIVERSITY®

Supported in part by the  
U.S. DEPARTMENT OF  
**ENERGY** | Office of  
Science

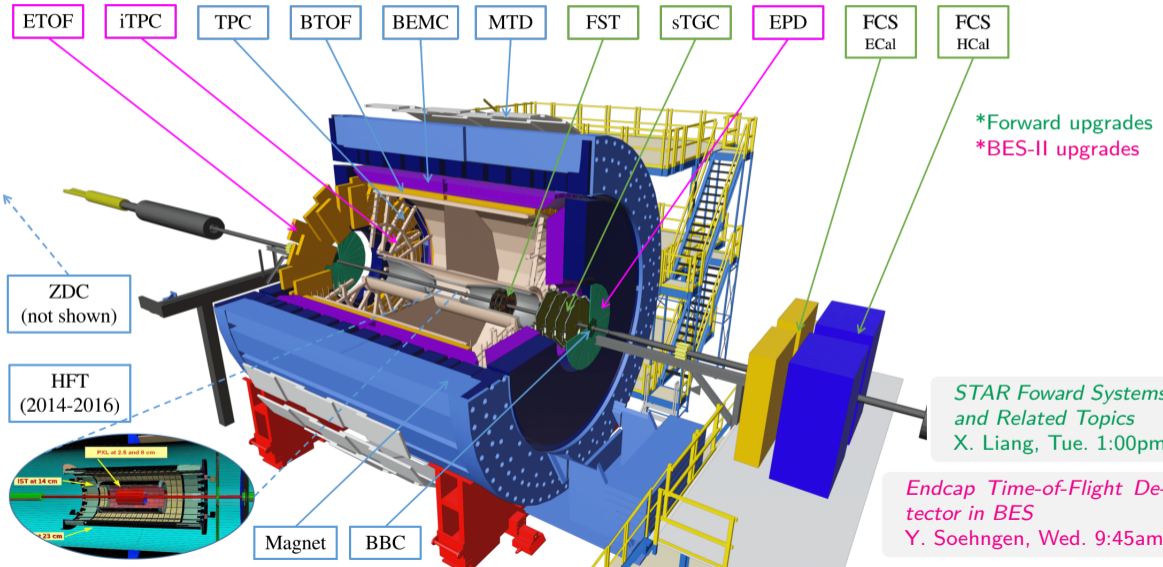
2024 RHIC/AGS ANNUAL USERS' MEETING

**A New Era of Discovery**  
Guided by the New Long Range Plan  
for Nuclear Science

June 11–14, 2024



# STAR detector



\*Forward upgrades  
\*BES-II upgrades

STAR Forward Systems and Related Topics  
X. Liang, Tue. 1:00pm

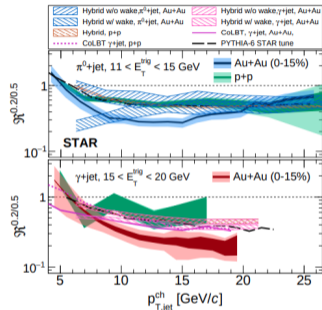
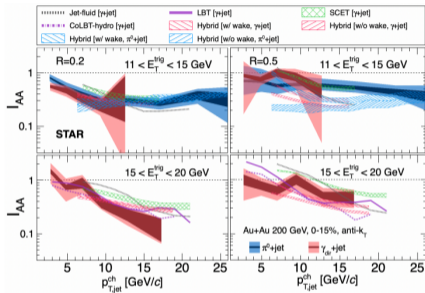
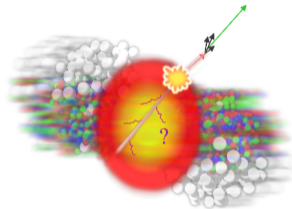
Endcap Time-of-Flight Detector in BES  
Y. Soehngen, Wed. 9:45am

# Outline

1. Jet & Heavy Flavor
2. Flow
3. QCD critical point search
4. Chirality/Vorticity
5. Hyperon-nucleon interaction

# Jet modification

[STAR, arXiv:2309.00145,2309.00156]

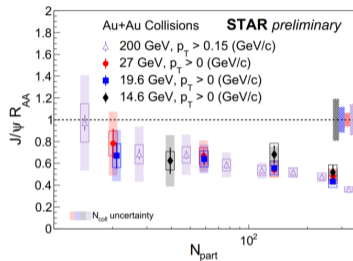


- ▶ recoil-jet yields per trigger ( $Y$ ) ratio Au+Au over p+p,  $I_{AA} < 1 \rightarrow$  medium-induced yield suppression  $\rightarrow$  jet quenching
- ▶ greater suppression in smaller “jet radius”  $R \rightarrow$  jet broadening

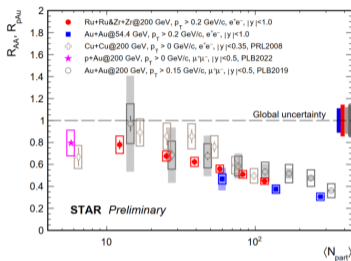
$$I_{AA} = \frac{Y^{\text{Au+Au}}(p_{T,\text{jet}}^{\text{ch}}, R)}{Y^{\text{p+p}}(p_{T,\text{jet}}^{\text{ch}}, R)}$$

$$\mathfrak{R}^{\frac{\text{small-}R}{\text{large-}R}} = \frac{Y^{\text{A+A}}(p_{T,\text{jet}}^{\text{ch}}, \text{small } R)}{Y^{\text{A+A}}(p_{T,\text{jet}}^{\text{ch}}, \text{large } R)}$$

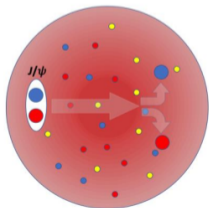
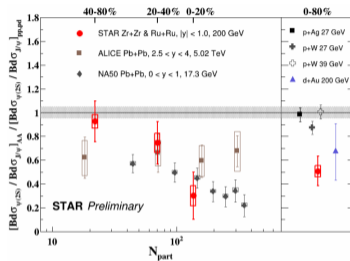
### $J/\psi$ energy dependence



### $J/\psi$ system size dependence

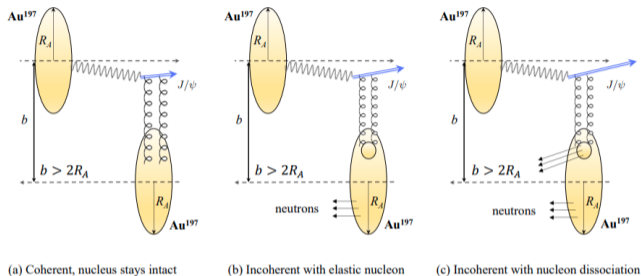


### $\psi(2s)$ over $J/\psi$ ratio



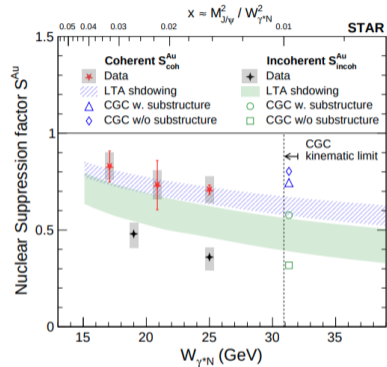
- ▶ No significant energy or system dependence
- ▶  $\psi(2s)$  over  $J/\psi$  double ratio  $< 1 \rightarrow$  sequential suppression

# $J/\psi$ photoproduction in UPC



[STAR, arXiv:2311.13637, arXiv:2311.13632]

- ▶ At photon-nucleon center-of-mass energy  $W_{\gamma^*N}$  of 25 GeV, the coherent and incoherent  $J/\psi$  cross sections of Au nuclei are found to be  $(71 \pm 10)\%$  and  $(36 \pm 7)\%$ , respectively, of that of free protons.
- ▶ comparison with models  $\rightarrow$  possible shadowing effect, color glass condensate



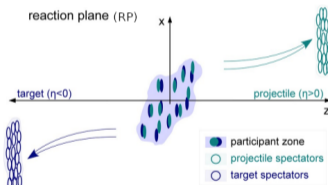
$S^{\text{Au}}$ : ratio between  $J/\psi$  cross section and the impulse approximation (IA). IA neglects all nuclear effects except for coherence.

# Outline

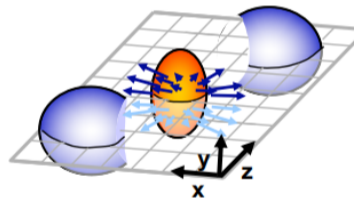
1. Jet & Heavy Flavor
2. Flow
3. QCD critical point search
4. Chirality/Vorticity
5. Hyperon-nucleon interaction

Flow: the collective motion of produced particles

$$\frac{dN}{d\phi} \propto 1 + \sum_{n=1} 2v_n \cos n(\phi - \Psi_{RP})$$



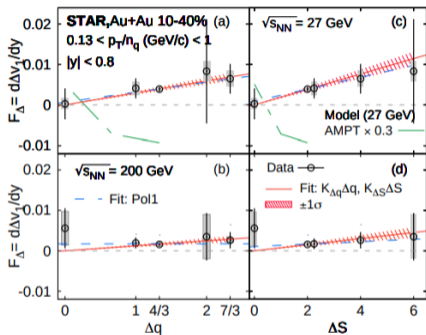
direct flow ( $v_1$ )



elliptic flow ( $v_2$ )

# $\Delta v_1$ combination dependence on charge and strangeness

A. Iktal, Tue. 4:00pm  
A. Dash, Wed. 4:30pm



$\Delta q$	$\Delta S$	$\Delta v_1$ combination
0	0	$[\bar{p}(\bar{u}\bar{u}\bar{d}) + \phi(s\bar{s})] - [K^-(\bar{u}s) + \bar{\Lambda}(\bar{u}\bar{d}\bar{s})]$
1	2	$[\bar{\Lambda}(\bar{u}\bar{d}\bar{s})] - [\frac{1}{3}\Omega^-(sss) + \frac{2}{3}\bar{p}(\bar{u}\bar{u}\bar{d})]$
$\frac{4}{3}$	2	$[\bar{\Lambda}(\bar{u}\bar{d}\bar{s})] - [K^-(\bar{u}s) + \frac{1}{3}\bar{p}(\bar{u}\bar{u}\bar{d})]$
2	6	$[\bar{\Omega}^+(\bar{s}\bar{s}\bar{s})] - [\Omega^-(sss)]$
$\frac{7}{3}$	4	$[\bar{\Xi}^+(\bar{d}\bar{s}\bar{s})] - [K^-(\bar{u}s) + \frac{1}{3}\Omega^-(sss)]$

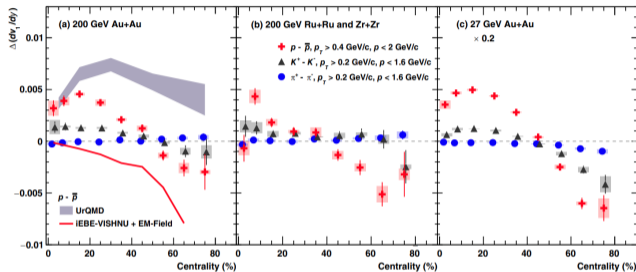
[STAR, arXiv:2304.02831]

- ▶  $K^-, \bar{p}, \bar{\Lambda}, \phi, \bar{\Xi}^+, \Omega^-, \bar{\Omega}^+ \rightarrow$  no  $u, d$  quarks  $\rightarrow$  no transported quarks
- ▶ assuming coalescence  $\rightarrow d\Delta v_1/dy \propto \Delta q, \Delta S$
- ▶ qualitatively consistent with Hall effect (Hall  $\gg$  Faraday+Coulomb) in 10-40% centrality



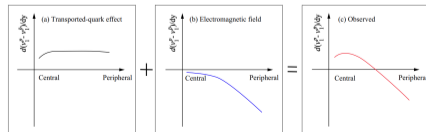
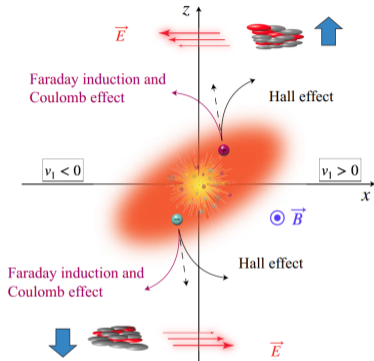
# $v_1$ splitting and possible EM effect

D. Shen, Tue. 9:25am  
A. Dash, Wed. 4:30pm

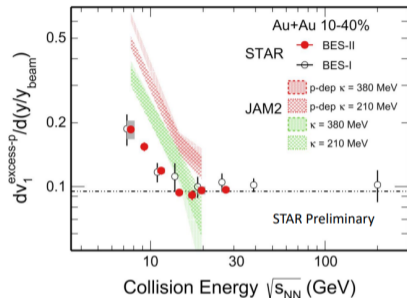
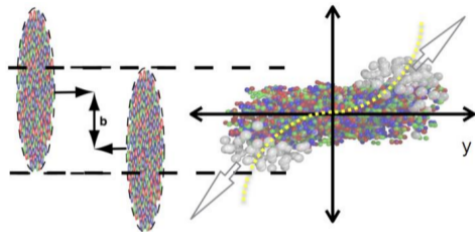


[STAR, PRX 14(2024)011028]

- ▶ particle-antiparticle  $v_1$  splitting  $d\Delta v_1/dy$
- ▶ pion, kaon, proton  $\rightarrow$  qualitatively interpreted by transported quark + electromagnetic field (Hall < Faraday+Coulomb) in peripheral collisions.



Other possibility: baryon inhomogeneities? [arXiv:2305.08806]

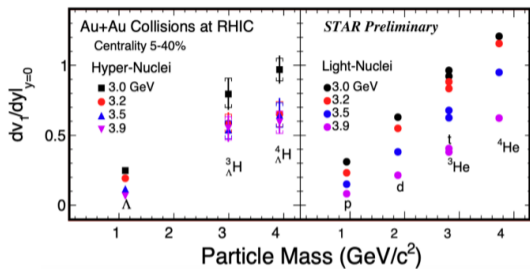


$$N_p v_{1,p} = N_p v_{1,\text{medium}} + (N_p - N_{\bar{p}}) v_{1,\text{excess}}$$

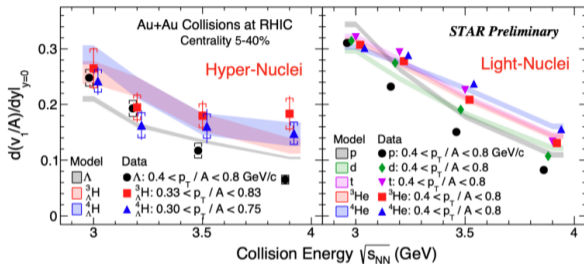
assuming  $v_{1,\text{medium}} = v_{1,\bar{p}}$

$$v_{1,\text{excess}} = \frac{v_{1,p} - v_{1,\bar{p}}}{1 - N_{\bar{p}}/N_p}$$

- ▶ BES-II: higher precision than BES-I
- ▶  $\sqrt{s_{NN}} > 11.5$  GeV flat scale;  $\sqrt{s_{NN}} \leq 11.5$  GeV deviate  $\rightarrow$  change in medium/collision dynamics
- ▶ Mean field model predicts the trend at low  $\sqrt{s_{NN}}$ , but higher  $\rightarrow$  data to constraint model EOS



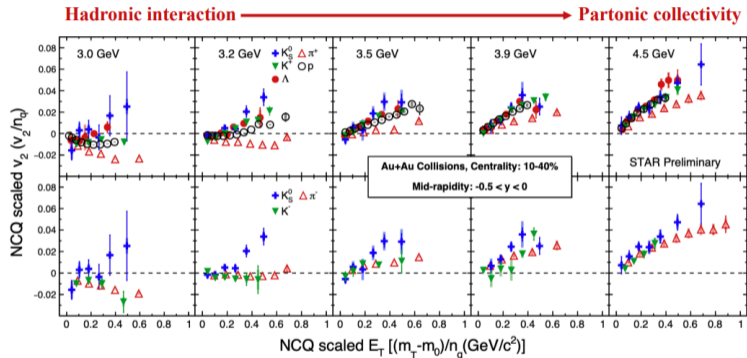
[STAR, PRL 130(2023)211301]



- ▶  $dv_1/dy$  scales with mass number
- ▶  $\sqrt{s_{NN}} \downarrow \rightarrow \mu_B \uparrow \rightarrow$  light and hyper nuclei abundance  $\uparrow$
- ▶  $\sqrt{s_{NN}} \downarrow \rightarrow d(v_1/A)/dy \uparrow$
- ▶ JAM2 mean field + coalescence calculations explains the energy dependence

# $v_2$ at FXT – breaking of NCQ scaling

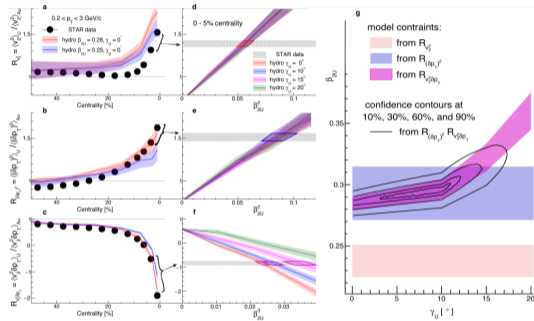
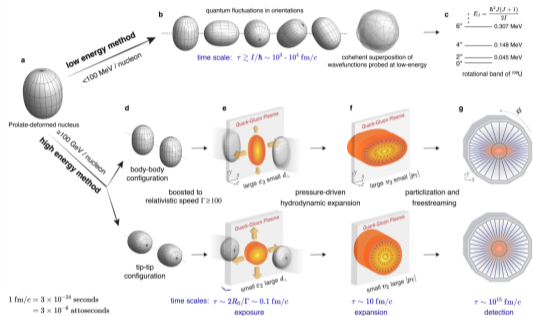
P. Sinha, Tue. 10:45am  
E. Duckworth, Tue. 3:00pm



partonic collectivity  
 → NCQ scaling: number of constituent quark scaling  
 → hadron flows follow the same scaling  $\frac{v_2}{n_q}$  vs.  $\frac{m_T - m_0}{n_q}$   
 or  $\frac{v_2}{n_q}$  vs.  $\frac{p_T}{n_q}$

▶ NCQ scaling breaks at  $\sqrt{s_{NN}} \leq 3.2$  GeV → shadowing effect + hadronic interaction

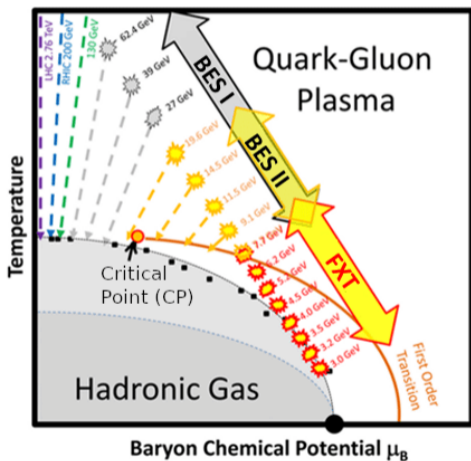
[STAR, arXiv:2401.06625]



- ▶ Nuclear surface shape  $R(\theta, \phi) = R_0(1 + \beta_2[\cos \gamma Y_{2,0} + \sin \gamma Y_{2,2}])$
- ▶ Central U+U/Au+Au ratio of  $\langle v_2^2 \rangle$ ,  $\langle (\delta p_T)^2 \rangle$ ,  $\langle v_2^2 \delta p_T \rangle$  data  $\rightarrow$  nonflow estimate/subtraction  $\rightarrow$  compare to hydro (IP-Glasma+MUSIC)  $\rightarrow$  estimate U nuclear shape parameter  $\beta_{2U}$

# Outline

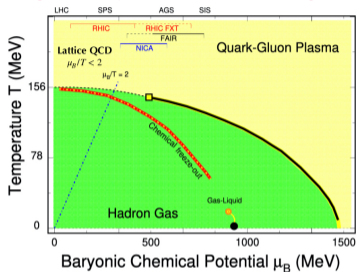
1. Jet & Heavy Flavor
2. Flow
3. QCD critical point search
4. Chirality/Vorticity
5. Hyperon-nucleon interaction



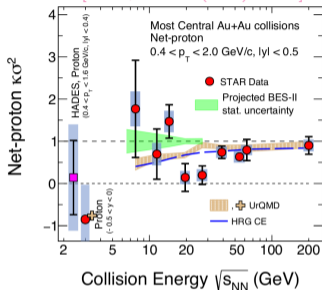
# Net-proton fluctuation in BES-II

Y. Huang, Wed. 2:30pm  
B. Mondal, Poster

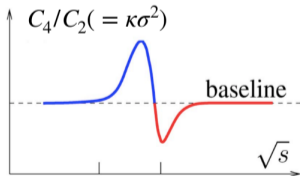
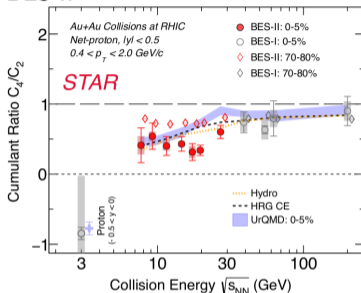
[B. Mohanty, N. Xu, arXiv:2101.09210]



BES-I [STAR, PRL 126(2021)092301]



BES-II

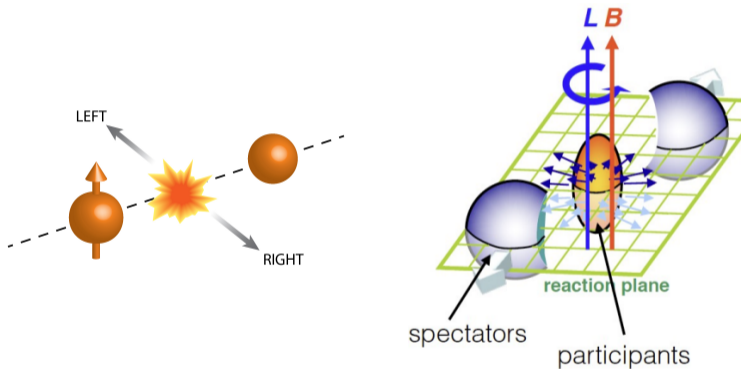


- ▶ QCD critical point (CP) is one of the most important physics
- ▶  $n$ : net-proton multiplicity in an event;  
 $\delta n = n - \langle n \rangle$ ;  $C_2 = \langle \delta n^2 \rangle$ ;  $C_4 = \langle \delta n^4 \rangle - 3\langle \delta n^2 \rangle^2$
- ▶ non-monotonic behavior expected around critical point
- ▶ BES-II  $\rightarrow$  measurements with higher precision compared to BES-I
- ▶  $C_4/C_2$  in 0-5%  $\rightarrow$  deviation from 70-80% and non-CP models  $\sim 20$ GeV

[M. Stephanov, PRL 107(2011)052301]

# Outline

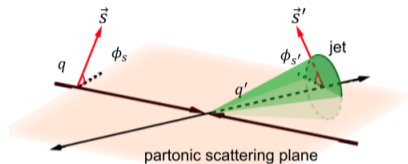
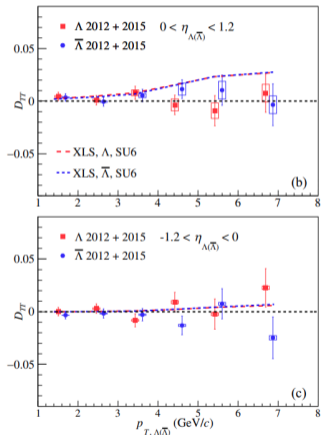
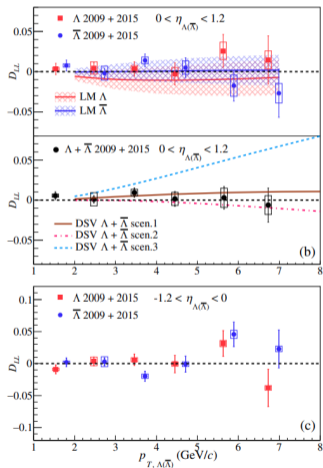
1. Jet & Heavy Flavor
2. Flow
3. QCD critical point search
4. Chirality/Vorticity
5. Hyperon-nucleon interaction





# Spin transfer to $\Lambda$ from polarized $p+p$ at 200 GeV

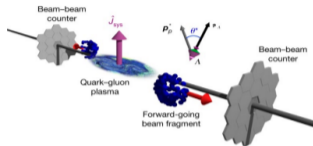
[STAR, PRD 109(2024)012004]



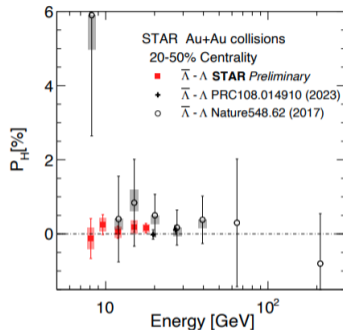
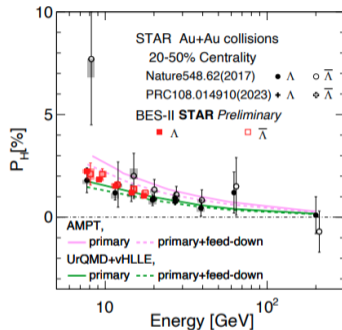
- ▶  $D_{LL}$  longitudinal spin transfer rate from polarized  $p$  to  $\Lambda(\bar{\Lambda})$
- ▶  $D_{TT}$  transverse spin transfer rate from polarized  $p$  to  $\Lambda(\bar{\Lambda})$
- ▶ consistent with models  $\rightarrow$  helpful to understand the spin structure of nucleons and hyperons

# $\Lambda$ global polarization

STAR, Nature 548 (2017) 62



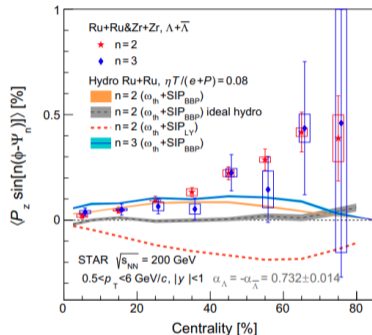
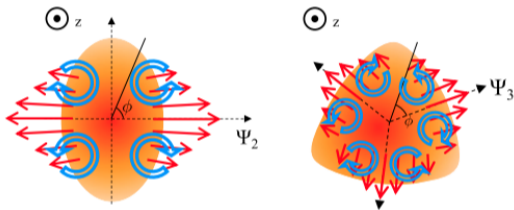
Courtesy of P. Tribedy



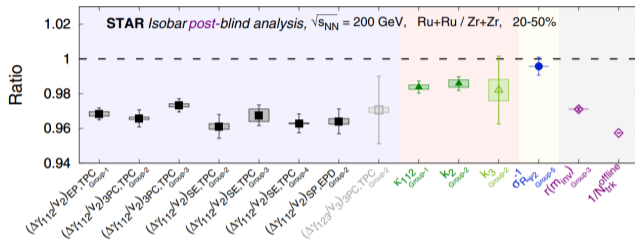
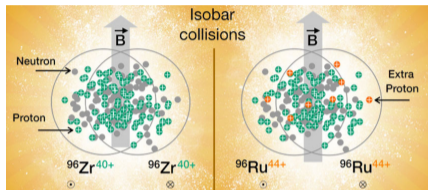
- ▶ updates of BES-II  $\sqrt{s_{NN}} = 7.7 - 17.3$  GeV with high precision
- ▶  $\Lambda$ ,  $\bar{\Lambda}$  opposite magnetic moment  $\rightarrow \vec{B}$  field enhances  $P_{\bar{\Lambda}}$  and reduce  $P_{\Lambda} \rightarrow$  splitting expected
- ▶ No splitting is observed within uncertainties between  $\Lambda$  and  $\bar{\Lambda}$  global polarization

# $\Lambda$ local polarization

[STAR, PRL 131(2023)202301]



- ▶  $\Lambda$  polarization along beam has dependence on azimuth w.r.t. EP  $\rightarrow$  vorticity pattern expected due to elliptic and triangular anisotropic flow
- ▶ comparison with models  $\rightarrow$  measurements provide stringent constraints on the thermal vorticity and shear-induced contributions to hyperon polarization

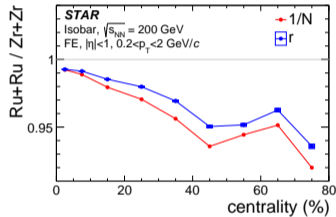


- ▶ **Chiral Magnetic Effect (CME):** magnetic field + chirality anomaly from QCD vacuum fluctuation  $\rightarrow$  charge separation phenomenon
- ▶ **Initial expectation:**  ${}^{96}_{44}\text{Ru}$ ,  ${}^{96}_{40}\text{Zr}$ : same  $A$ , different  $Z \rightarrow$  same background, different signal  
Ru+Ru: proton number  $\uparrow \rightarrow$  magnetic field  $\uparrow \rightarrow$  CME signal  $\uparrow \rightarrow \Delta\gamma/v_2 \uparrow \rightarrow \text{Ru/Zr} > 1$
- ▶ **STAR blind analysis** [STAR, PRC 105(2022)014901]  $\rightarrow$  isobar ratios Ru/Zr  $< 1$ , opposite to the initial expectation  $\leftarrow$  multiplicity diff.  $\leftarrow$  nuclear structure [Xu et al., PRL121(2018)022301].

# Isobar post-blind analyses for the CME

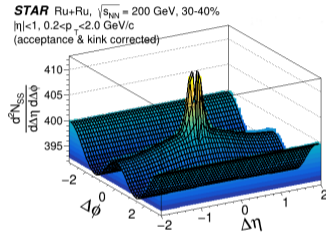
flow-induced backgrounds:

resonance decays  $\rightarrow$  estimated by pair excess  $r = \frac{N_{OS} - N_{SS}}{N_{OS}}$



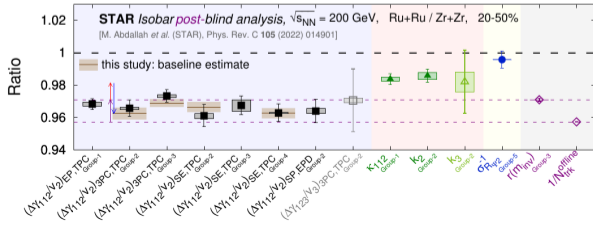
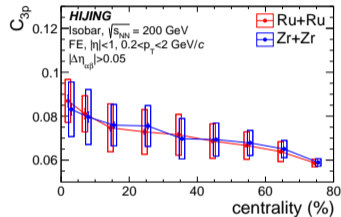
nonflow in  $v_2$  measurement:

fit two-particle  $(\Delta\eta, \Delta\phi)$  2D distribution to decompose



3-particle nonflow:

HIJING model  $\rightarrow$  no flow  $\rightarrow$  solely 3p nonflow bkg



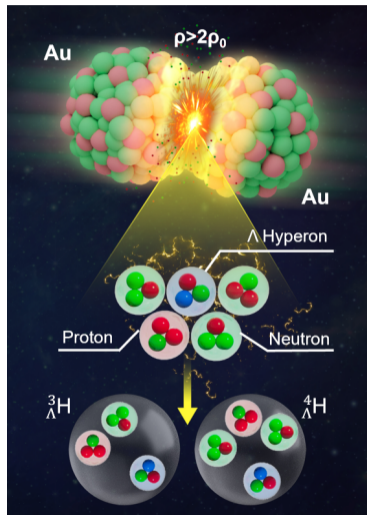
► **Post-blind:** nonflow background baseline estimate  $\rightarrow$  CME upper limit 10% (95% CL)

[STAR, arXiv:2308.16846, 2310.13096] .

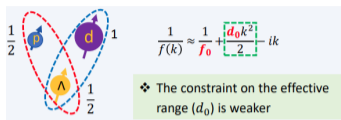
► CME is one of the most important physics of the field. Nonflow removal is critical towards final signal characterization.

# Outline

1. Jet & Heavy Flavor
2. Flow
3. QCD critical point search
4. Chirality/Vorticity
5. Hyperon-nucleon interaction



# $p/d - \Lambda$ correlations in Au+Au at 3 GeV



Correlation Function (CF):

$$C(\mathbf{k}^*) = \mathcal{N} \frac{\text{same event dist. for } \mathbf{k}^*}{\text{mixed event dist. for } \mathbf{k}^*}$$

Lednicky-Lyuboshitz (L-L) Approach

- ▶ modeling

$$C(\mathbf{k}^*) = \int d^3\mathbf{r}^* S(\mathbf{r}^*) |\Psi(\mathbf{r}^*, \mathbf{k}^*)|^2$$

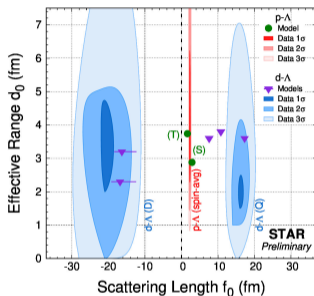
- ▶ S-wave assumed

$$\Psi(\mathbf{r}^*) = e^{-i\mathbf{r}^* \cdot \mathbf{k}^*} + \frac{f(\mathbf{k}^*)}{r^*} e^{i\mathbf{r}^* \cdot \mathbf{k}^*}$$

$$f(\mathbf{k}^*) \approx \left( \frac{1}{f_0} + \frac{d_0 \mathbf{k}^*}{2} - i\mathbf{k}^* \right)^{-1}$$

- ▶ Gaussian emission source assumed

$$S(\mathbf{r}^*) = (2\sqrt{\pi}R_G)^{-3} e^{-\mathbf{r}^{*2}/(4R_G^2)}$$



$p - \Lambda$  spin-average (fm)

$$f_0 = 2.32^{+0.12}_{-0.11}, d_0 = 3.5^{+2.7}_{-1.3}$$

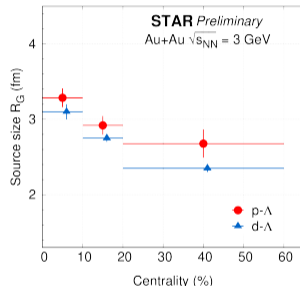
$d - \Lambda$  mixed with 2 states (fm)

$${}^2S_{1/2} \text{ (D): } f_0 = -20^{+3}_{-3}, d_0 = 3^{+2}_{-1}$$

$${}^4S_{3/2} \text{ (Q): } f_0 = 16^{+2}_{-1}, d_0 = 2^{+1}_{-1}$$

assuming Gaussian source  $S$

→ source size  $R_G$



$\mathbf{k}^*$  momentum in pair rest frame

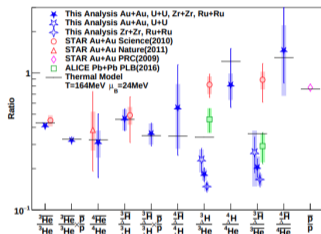
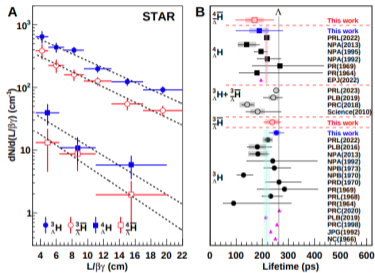
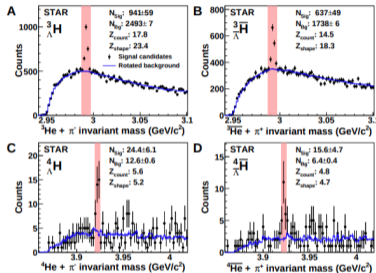
$f_0$  scattering length

$d_0$  effective range

# Hypernuclei production – first observation of $\frac{4}{\Lambda}\bar{H}$

I. Vassiliev, Wed. 10:30am

[STAR, arXiv:2310.12674]



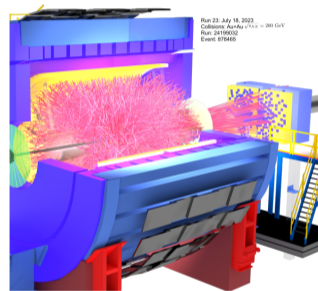
- ▶ First observation of antimatter hypernucleus  $\frac{4}{\Lambda}\bar{H}$
- ▶ Measurements of  ${}^3_{\Lambda}H$ ,  ${}^3_{\Lambda}\bar{H}$ ,  ${}^4_{\Lambda}H$ ,  ${}^4_{\Lambda}\bar{H}$  yields and lifetimes.
- ▶ Yield ratios  $\rightarrow$  consistent with thermal model and previous publications.

datasets:  
Au+Au 200GeV  
Ru+Ru, Zr+Zr, 200GeV  
U+U 193GeV



# Summary and Outlook

- ▶ STAR continues producing results of great impact for important physics on QCD
- ▶ Many new analyses ongoing
- ▶ Fully upgraded STAR detector
  - BES and forward upgrades in operation since 2022
  - Run 23 was the 1<sup>st</sup> top energy Au+Au with all upgrades
- ▶ Unprecedented high statistics Au+Au/p+p/p+Au data in 2023-25



[STAR, BUR Runs 24-25]

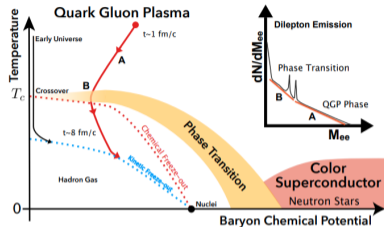
# Backup

Previous STAR highlights

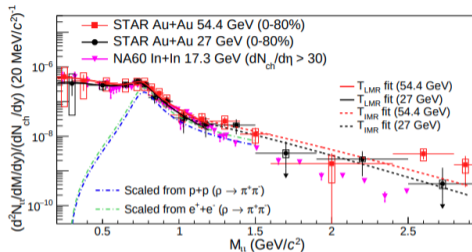
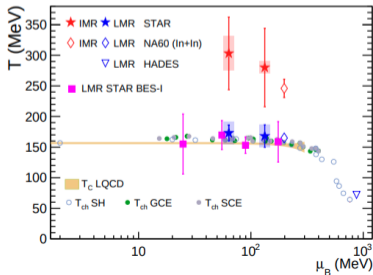
▶ AUM2023

▶ AUM2022

# QGP temperature estimate from dielectron spectra

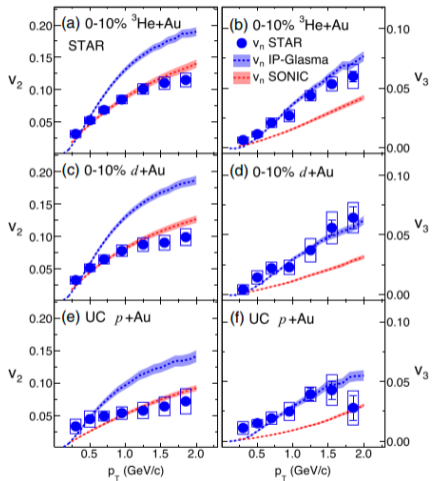


[STAR, arXiv:2402.01998]



← thermal dielectrons (decay bkgd's removed, except for  $\rho^0$ )

- ▶ low-mass region (LMR):  $\rho^0$  dissolved in QGP, closer the phase transition  $\rightarrow$  fit by  $\rho^0$  decay Breit-Wigner  $f^{BW}$  with Boltzmann factor  $e^{-M/k_B T} \rightarrow T_{LMR}$ 
  - measurements (STAR: BES-I, BES-II; NA60; HADES) consistent with LQCD calculation and thermal models
- ▶ intermediate-mass region (IMR): earlier in QGP  $\rightarrow$  fit by Boltzmann function  $\rightarrow T_{IMR}$ 
  - $T_{IMR} > T_{LMR}$



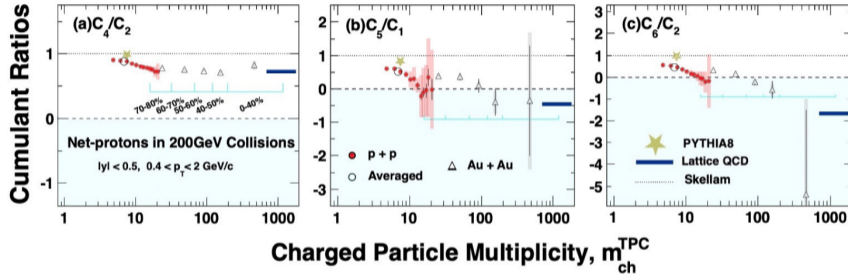
- ▶  $v_2(p_T)$  dependent on the colliding systems,  $v_3(p_T)$  system-independent
- ▶  $v_2(p+\text{Au}) < v_2(d+\text{Au}, ^3\text{He}+\text{Au})$   
→ sub-nucleonic eccentricity fluctuations

[STAR, PRL 130(2023)242301]

[STAR, arXiv:2312.07464]

# Net-proton fluctuation in p+p at $\sqrt{s_{NN}} = 200$ GeV

[STAR, arXiv:2311.00934]



- ▶ ratios below the expectations of Skellam distribution
- ▶ PYTHIA8 calculations fail to reproduce those ratios
- ▶ connecting to Au+Au results at 200 GeV